

Mode-Coupling Control and New Index Profile of GI POF for Restricted-Launch Condition in Very-Short-Reach Networks

Takaaki Ishigure, *Member, IEEE*, Kunihiro Ohdoko, Yorichika Ishiyama, and Yasuhiro Koike, *Member, IEEE*

Abstract—This paper confirms that numerical aperture (NA) is a key factor in mode coupling [the energy transfer among propagating modes in multimode fibers (MMF)] and that providing a high NA is a viable solution to reduce mode coupling in graded-index plastic optical fibers (GI POFs). Furthermore, the authors propose a new refractive-index-profile design of GI POFs when only small mode groups are launched (restricted-launch condition), which is a combined profile with the index exponents lower and higher than optimum value for the core center and periphery, respectively. The advantage of the new index profile is investigated both experimentally and theoretically. Furthermore, it is verified that the high-bandwidth performance of GI POF with the new index profile under the restricted-launch condition is maintained even when statistical fiber bendings are added to the GI POF and when misalignment is caused at the optical coupling between the light source and the GI POF.

Index Terms—Graded-index plastic optical fiber (GI POF), mode coupling, numerical aperture (NA), restricted-launch condition.

I. INTRODUCTION

THE EXPLOSIVE spread of the Internet has given us a highly developed broadband-network society. In order to meet the demand of large-scale and interactive communication services, improvements are required in the architecture and data rates of whole networks.

Silica-based single-mode optical fibers are widely utilized in long-distance backbone-networks transmission on the order of 10 Gb/s because of its high bandwidth and low attenuation. In recent years, silica-based multimode fibers (MMFs) have become popular for Gigabit Ethernet and 10-Gb Ethernet [1]. The large core diameter of silica-based MMF (50 or 62.5 μm) relaxes the tolerance required in connections between fiber-to-fiber and fiber-to-light sources and detectors, compared with those in single-mode fiber (5 \sim 10- μm diameter) links.

On the other hand, plastic optical fibers (POFs) with much larger cores (120 \sim 1000 μm) than silica fibers are expected to be a communication medium in middle- or short-distance networks (300 \sim 100 m) [2]–[4], because its large core and great mechanical flexibility allow for easy network installation,

which can dramatically decrease the total system cost. We have proposed a high-bandwidth graded-index (GI) POF that has a quadratic refractive-index profile in the core region, and have improved its bandwidth characteristics [5]. Moreover, we have designed an optimum-index profile of GI POF for transmitting greater than gigabit data rates [6]. Because large-core POF propagates more than 10 000 modes, modal-dispersion management is a key technology. We have already demonstrated not only modal-dispersion management by the refractive-index-profile control, but also the improvement of the material dispersion of polymers by a perfluorinated POF [5]–[8]. In addition to the dispersion-management techniques, the propagating-mode analysis and the management of propagating-mode characteristics in the GI POF are also serious issues because it is well known that the mode coupling (the energy transfer among the propagating modes) in MMFs strongly influences the fiber bandwidth. In step-index (SI)-type POFs, large mode coupling has been experimentally observed [9], [10], while we have proven that the mode-coupling effect on the bandwidth in GI POF is smaller than that in SI POF [11]. Regarding the origin of the mode coupling, several hypotheses such as large scattering or perturbation of the waveguide properties have been proposed [11]–[13]. However, those are only for silica-based MMFs, and there are few proposals for GI POF. In this study, we confirm that NA is a key factor in the mode-coupling strength, and that providing high NA is a viable solution for reducing mode coupling in GI POF. In such a high-NA GI POF with small mode coupling, the launch condition is an important issue for its bandwidth performance. Therefore, a new index-profile design of GI POFs when only small mode groups are launched (restricted-launch condition) is proposed, because the restricted-launch condition is expected in a real high-speed GI POF link. Then, the high-bandwidth performance of the GI POF with the new index profile is confirmed experimentally and theoretically. Furthermore, the stability of high-bandwidth transmission under physical perturbations expected in very-short-reach networks is also investigated.

II. EXPERIMENTAL

A. Fiber Preparation

The GI POF is obtained by heat-drawing a preform in which the GI profile is already formed. A detailed fabrication method of the GI POF is described in [5], [6], and [8]. We can control the refractive-index profile of the GI POF by changing the

Manuscript received January 19, 2005; revised June 8, 2005.

T. Ishigure, Y. Ishiyama, and Y. Koike are with the Faculty of Science and Technology, Keio University, Yokohama 223-8522, Japan, and Japan Science and Technology Agency (JST) Exploratory Research for Advanced Technology (ERATO), Kawasaki 212-0054, Japan (e-mail: ishigure@appi.keio.ac.jp).

K. Ohdoko is with Sumitomo Mitsui Banking Corporation (SMBC) Consulting Company, Ltd., Chiyoda-ku, Tokyo 102-0082, Japan.

Digital Object Identifier 10.1109/JLT.2005.859427

polymerization temperature and composition of the polymerization initiator and the chain transfer agent in the interfacial-gel polymerization process. Furthermore, we can also control the NA by changing the concentration of the dopant (diphenyl sulfide) that has a refractive index ($n_d = 1.629$) higher than that of poly-methyl-methacrylate (PMMA) ($n_d = 1.492$) for the core polymerization. We fabricate GI POFs with various refractive-index profiles and NAs to investigate the bandwidth and propagating-mode characteristics. In this paper, the core and fiber diameters are controlled in the heat-drawing process to be 400 or 500 μm , and 600 or 750 μm , respectively.

B. Refractive-Index Distribution and Dispersion Analysis

The refractive-index profiles formed in the core region of multimode optical fibers play a great role in determining their bandwidth, because modal dispersion is generally dominant in MMFs. We have reported that the GI POF prepared by the interfacial-gel polymerization process enables greater than gigabit data transmission [5]–[8]. Furthermore, we have analyzed the bandwidth potential of GI POFs by taking all modal, material, and profile dispersions into account. Material and profile dispersions are induced by the wavelength dependence of the refractive index of fiber materials. For instance, in the case of PMMA-based GI POFs, we have shown theoretically that the large material dispersion limits the maximum bandwidth to be approximately 3 GHz for a 100-m distance at a wavelength of 0.65 μm when a light source with a 2-nm spectral width is used [8].

For such a bandwidth analysis of GI POF, it is necessary to quantitatively approximate the refractive-index profile of the GI POF. For designing the optimum index profile of GI POF, the approximation of the index profile by the well-known power-law form described by (1) is suitable.

$$n(r) = n_1 \left[1 - 2\Delta \left(\frac{r}{a} \right)^g \right]^{\frac{1}{2}}, \quad 0 \leq r \leq a$$

$$= n_2, \quad r \geq a \quad (1)$$

where n_1 and n_2 are the refractive indexes of the core center and cladding, respectively, a is the core radius, and Δ is the relative index difference defined as

$$\Delta = \frac{n_1^2 - n_2^2}{2n_1^2}. \quad (2)$$

The parameter g , called the index exponent, determines the refractive-index profile.

The refractive-index profile of GI POF is experimentally measured by the transverse interferometric technique [14]. We have already confirmed that this method has the highest accuracy in measuring the graded refractive-index distribution formed in such a wide area. However, for analyzing the bandwidth of the experimentally obtained GI POF, it was found that the power-law form shown by (1) could not precisely represent the measured refractive-index profile [7], [8], [11]. Therefore, the approximation of the index profile by a ten-term polynomial function of distance r from the center axis of the

fiber as shown in (3) is also adopted for quantitative dispersion analysis.

$$n(r) = n_1 \left[1 - 2 \cdot \Delta \cdot \left\{ A_{10} \cdot \left(\frac{r}{a} \right)^{10} + A_9 \cdot \left(\frac{r}{a} \right)^9 + \dots + A_2 \cdot \left(\frac{r}{a} \right)^2 + A_1 \cdot \left(\frac{r}{a} \right) \right\} \right]^{\frac{1}{2}} \quad (3)$$

where $A_{10}, A_9, \dots, A_2, A_1$ are constants independent of the wavelength of transmission. By introducing this approximation method, it becomes possible to precisely approximate the experimentally measured index profile [11].

For designing the ideal index profile of GI-type MMF, the power-law form shown by (1) has been useful, because there is only one parameter determining the index profile. In this paper, the power-law form is used only for visualizing the deviation of the index profile from the optimum ($g = 2.4$).

By approximating the index profile by (3), the dispersion characteristics of each mode in the GI POF can be theoretically estimated. In this study, the Wentzel-Kramers-Brillouin (WKB) numerical-computation process [15] is adopted, and the calculated results are compared with those experimentally measured by the differential-mode-delay (DMD) method, which is described in Section II-C.

C. Bandwidth Measurement of the GI POF

The bandwidth of GI POFs is measured by a time-domain-measurement method, in which an optical pulse was launched onto the fiber by an InGaAlP laser diode (LD) at 0.65 μm . The input optical pulse created by a pulse generator is coupled into the GI POF, and the output pulse is measured with an optical sampling oscilloscope (Hamamatsu C-8188-03). The bandwidth of the oscilloscope is as high as 3 GHz, and the detection part of the optical pulse is designed for collecting all optical signals emerging from large-core POFs ($\sim 1\text{-mm}$ core diameter). Due to a special modulation process for obtaining a narrow optical pulse with a width of 50 ps [full width at half maximum (FWHM)], the spectral width of the signal is as broad as 3 nm. After measuring the waveforms of input and output pulses, the -3-dB bandwidth of the GI POF is calculated from the Fourier transform of these waveforms.

The launch condition of GI POF is a very important issue in the measurement of the bandwidth. Generally, in bandwidth measurements of multimode silica fibers, as advocated in several previous works [16], a steady-state mode-power distribution should be established when MMFs are intended to be adopted in long-haul telecommunication networks. This is because the use of MMF in the long-distance link formed the steady-state mode-power distribution. Also, the use of an LED as a light source had been considered since the 1980s. In this paper, a short SI POF (1-m length, 980- μm core diameter, NA of 0.5) is used as the mode exciter to establish the uniform launching conditions of all modes [we define this condition as the overfilled launch condition: (OFL) of GI POF]. A pulsed signal (approximately 50 ps at FWHM) is directly launched into the 1-m SI POF followed by the tested

GI POF sample by butt-coupling on a V-groove. Since the power distribution at the output end of the 1-m SI POF is uniform in its core region ($980\ \mu\text{m}$), which have been already confirmed in [11], and the numerical aperture (NA) of the SI POF (0.5) is sufficiently higher than that of the GI POF (0.15–0.3), the 1-m SI POF is considered as an ideal mode exciter for a uniform launch. On the other hand, for practical use in a high-speed optical link, an LD or vertical-cavity surface-emitting laser (VCSEL) will be used. As the VCSEL generally excites only small mode groups in the MMFs [17], [18] because of its small radiation angle and radiating area, particularly in GI POF with a much larger core diameter than silica-based MMF, only low-order modes would be excited by a small spot and narrow divergence angle of a VCSEL focused on the core center of GI POF. Thus, the bandwidth performance should be investigated under the restricted-launch condition. In this paper, we adopt the following restricted condition as the under-filled launch (UFL) condition: a $6.48\text{-}\mu\text{m}$ spot size and 0.16-NA beam is focused on the input end of a GI POF.

D. Propagating Modal Analysis

Even when GI POFs exhibit high bandwidth under the UFL condition, mode coupling can degrade the high-bandwidth performance. The mode-coupling strength in GI POFs is investigated by two methodologies: DMD, and the launch-condition dependence of the near-field pattern (NFP) [11].

The DMD measurement is carried out as follows: an optical pulse signal from an LD at $0.65\text{-}\mu\text{m}$ wavelength (pulse width is approximately 50 ps of FWHM) is coupled to a GI POF via a 1-m single-mode fiber that satisfies the single-mode condition at $0.65\ \mu\text{m}$ in order to launch a specified mode group of the GI POF. By scanning the position where the single-mode-fiber probe is butted to the GI POF, from the core center to the periphery, each mode group from low to high order can be selectively launched. Then, we measure the differences in the time of flight of optical pulses among the different mode groups by an optical sampling oscilloscope, similar to the bandwidth measurement mentioned in Section II-C.

We also measure the launch-condition dependence of the NFP from GI POFs with different NA. The methodology of the launch-condition-dependence measurement is similar to that of DMD measurement: an optical signal (not pulsed) from an LD at a wavelength of $0.65\ \mu\text{m}$ is coupled to a GI POF via a single-mode fiber with a length of 1 m in the same way as the DMD measurement. In this case, the two launch conditions (lowest and highest order mode groups) are selected, which are created by light couplings at the core center and near the boundary of the core and the cladding, respectively. Then, we measure the NFPs after 100-m GI POF transmissions with a charge-coupled-device (CCD) camera system (Hamamatsu LEPAS-11).

E. Stability of High-Bandwidth Performance Under Perturbations

The GI POF with the completely optimum profile ($g = 2.4$) in the whole core region is able to maintain its high-bandwidth

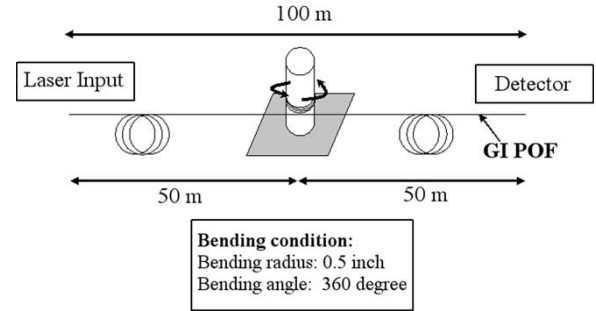


Fig. 1. Schematic representation of fiber-bending-test condition.

performance not only under the OFL condition but also under misalignment in launching under the UFL condition [8] and under static fiber bending, which causes mode coupling, as well. However, it is of great concern that the high-bandwidth performance under the UFL condition can be degraded in the case of the GI POF with an index profile that deviates from the optimum one due to such physical perturbations in the fiber.

Therefore, we initially measure the bandwidth variation when the launch-beam spot size and launch position are varied. The launch condition is varied by using a short-length (1 m) single-mode silica fiber and a short-length GI POF with $70\text{-}\mu\text{m}$ core diameter as a probe fiber for restricted launch. Basically, under the UFL launch condition, the launched-mode power distribution largely depends upon the light source and related optics in transmitters. In order to cover the variable-mode power distribution created by a wide variety of transmitters, we utilize the two different probe fibers, as mentioned above. A single-mode fiber can launch a limited number of modes, while a larger number of modes can be excited by the small-core ($70\ \mu\text{m}$) GI POF than by the single-mode-fiber probe. Here, the single-mode fiber used for the probe satisfies the single-mode condition even at a wavelength of $0.65\ \mu\text{m}$. To measure the launch-condition dependence of bandwidth, each fiber probe is butt-coupled to the GI POF, and the bandwidth performance is measured when the butted position is displaced in the same way as in the DMD measurement.

Furthermore, the effect of fiber bending on the bandwidth performance is also investigated. The fiber bending condition in this measurement is shown in Fig. 1. The 100-m GI POF is bent at a distance of 50 m (half of the transmission length) from the input by turning on a mandrel with 0.5-in diameter, and then, the number of turns on the mandrel is varied from zero to ten.

III. RESULTS AND DISCUSSION

A. NA Dependence of Mode-Coupling Strength

The launch-condition dependence of the NFPs of GI POFs with different NA (0.15, 0.17, 0.20, and 0.30) are shown in Fig. 2. As we have already demonstrated in [19], a significant profile difference between the low- and high-order modes is observed in the high-NA GI POF ($\text{NA} = 0.3$), while in the low-NA GI POF, the profiles are independent of the launch condition, as shown in Fig. 2. From the results of a wide variety of GI POFs measurements, a relationship between the mode-coupling strength and fiber NA is confirmed. It is also

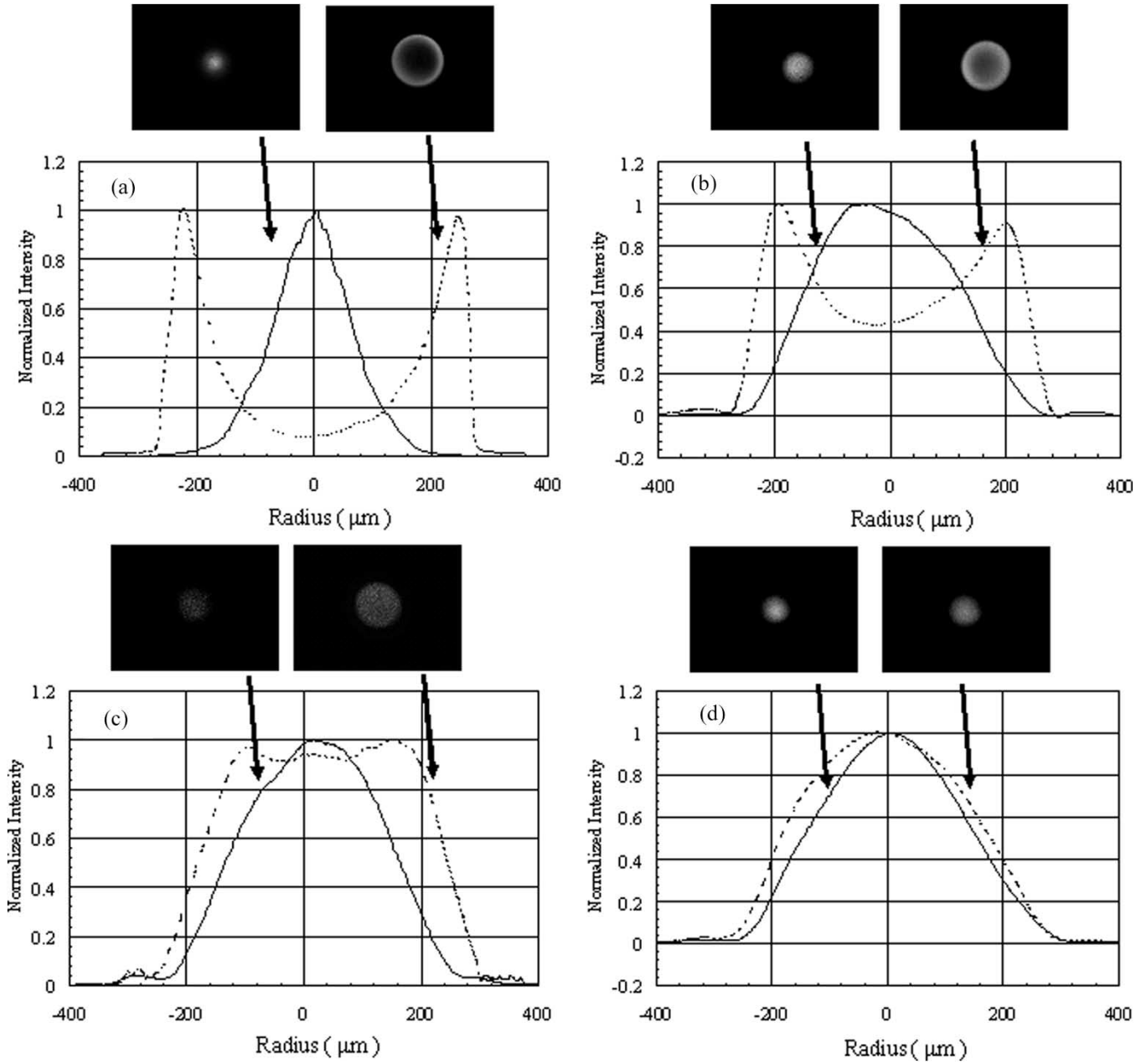


Fig. 2. Fiber NA dependence of NFPs of 100-m GI POF (NA: 0.15–0.30). 2-D photos and normalized power distribution in radial direction. Solid line: center launch. Broken line: peripheral launch (offset). (a) Fiber 1, NA = 0.30. (b) NA = 0.20. (c) NA = 0.17. (d) Fiber 2 NA = 0.15.

found that, as shown in Fig. 2, for an NA of more than 0.17, the launch-condition dependence of NFP becomes obvious in the GI POFs.

This NA dependence of the mode-coupling strength is analyzed quantitatively. It is found that the strength of the mode coupling can be related to the difference in the propagation constant ($\Delta\beta$) between the adjacent modes.

If the refractive-index profile of the GI POF can be approximated by the power-law form shown as (1), the propagation constant β of the mode whose principal mode number m is described by the following equation.

$$\beta = n_1 k \left[1 - 2\Delta \left(\frac{m}{M} \right)^{\frac{2g}{g+2}} \right]^{\frac{1}{2}} \quad (4)$$

where k is the wavenumber, and M is the maximum principal mode number. From (4), it can be derived that $\Delta\beta$, which is the difference between β of the modes with different m , is a function of n_1 and Δ . If two modes have the same propagation constants, namely $\Delta\beta = 0$, these modes are called degenerate modes. On the other hand, if the value of $\Delta\beta$ is large, the probability of energy transfer between these two modes decreases; thus little mode coupling can be observed. Therefore, large n_1 and Δ values are expected to decrease the mode coupling in the GI POF.

The fiber NA dependence of the $\Delta\beta$ values is calculated, and the results are shown in Fig. 3(a). Here, $\Delta\beta$ is defined as the propagation-constant difference of m th- and $(m + 5)$ th-order modes, since the large-core GI POF propagates a huge number

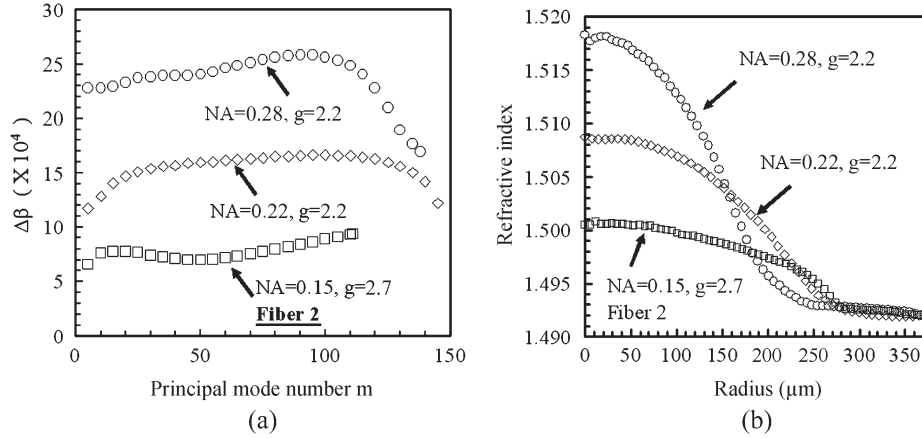


Fig. 3. (a) Fiber NA dependence of the difference between propagation constants ($\Delta\beta$) of adjacent modes. (b) Refractive-index profile of the GI POF used for the calculation of $\Delta\beta$ shown in (a).

TABLE I
COEFFICIENTS OF REFRACTIVE-INDEX-PROFILE APPROXIMATION BY TEN-TERM-POLYNOMIAL FORM

	A_{10}	A_9	A_8	A_7	A_6	A_5
Fiber 1	-2.977	5.320	0.356	-0.170	-5.131	2.243
Fiber 2	1.099	-1.237	-2.550	4.359	0.657	0.207
Fiber 3	-19.28	47.17	-20.70	-24.76	10.23	19.75
Fiber 4	-340.2	1134	-1392	719.6	-111.1	24.99
	A_4	A_3	A_2	A_1	n_1	$\Delta \times 10^{-3}$
Fiber 1	1.625	-1.108	0.862	0.011	1.521	18.8
Fiber 2	-5.856	4.302	0.073	-0.029	1.501	5.26
Fiber 3	-14.26	1.859	1.030	-0.039	1.516	16.2
Fiber 4	-61.24	33.62	-6.755	88.93	1.519	16.9

of modes. Each $\Delta\beta$ value was calculated from the refractive-index profile shown in Fig. 3(b). In this case, the refractive-index profile was approximated by the ten-term polynomial form as described by (3). By utilizing the polynomial form, we can accurately calculate the propagation constant β of the mode with arbitrary order with the WKB numerical-computation process [8], [15]. The polynomial-fitting parameters that have been used in the approximations are summarized in Table I. It can be seen that the $\Delta\beta$ values increase with increasing fiber NA. This is considered to be one of the reasons why small mode coupling is observed in the higher NA GI POF. Because both theoretical and experimental results show the same trend, it is verified that the NA is a key factor in mode-coupling strength, and that the amount of mode coupling can be controlled by adjusting the NA of GI POFs.

B. New Index-Profile Design of GI POFs

We prove in the above section that reduction of the mode coupling is possible in high-NA GI POFs. However, the modal dispersion of the GI POF is also strongly influenced by the fiber NA. If the refractive-index profile deviates slightly from the optimum profile, significant output-pulse distortion is observed for high-NA (0.25–0.30) GI POFs compared to the output pulses from low-NA GI POFs with the same index exponent. The experimentally measured refractive-index profiles of the

different NA GI POFs are shown in Fig. 4(a), and the output-pulse waveforms from these 100-m GI POFs under the OFL condition are shown in Fig. 4(b). These GI POFs have the same index-exponent value ($g = 2.9$) and are shown as open circles in Fig. 4(a). Although the measured refractive-index profiles of the two GI POFs are expressed by the same index exponent, a larger output-pulse broadening is observed in the high-NA GI POF, as shown in Fig. 4(b). This is because the modal dispersion in the high-NA GI POF is larger than that in the low-NA GI POF, despite the same index exponent. Furthermore, the high-order modes that have large group delay exhibit the attenuation lower than the higher order modes of low-NA GI POF. Hence, the high-order modes in high-NA GI POF largely contribute to the pulse broadening. Therefore, a perfectly optimal refractive-index profile is required for the high-NA GI POF to achieve high bandwidth, particularly when all the modes are equally launched (OFL).

On the other hand, even if the refractive-index profile is not completely optimized, high bandwidth is expected under the UFL condition mentioned above, when the mode-coupling effect is small enough. At first, we investigate the bandwidth of a PMMA-based GI POF with high NA (0.25 ~ 0.30). When the approximated index exponent ($g = 2.9$) is larger than the optimum value ($g = 2.4$) throughout the core region, as shown in Fig. 5(a) (fiber 3), the bandwidth under the OFL and UFL conditions of the 100-m fiber 3 at a wavelength of 0.65 μm were

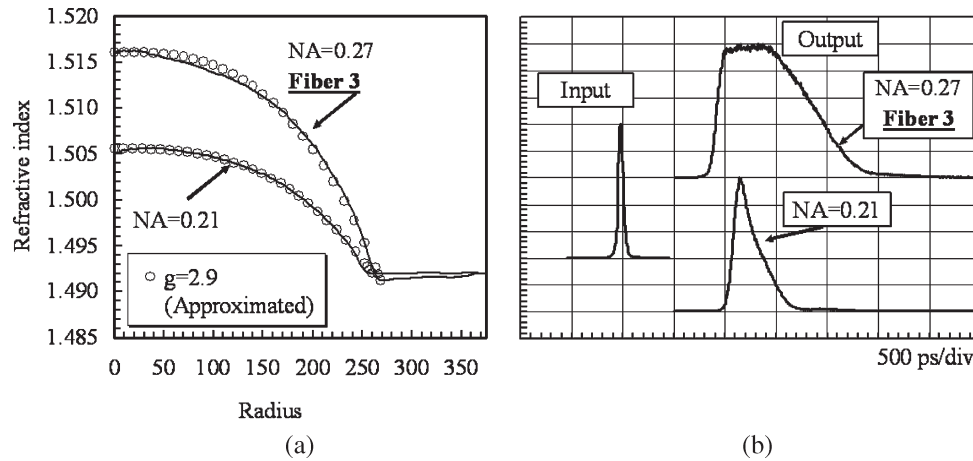


Fig. 4. Measured refractive-index profile and output-pulse waveforms from 100-m fiber 3 (NA = 0.27, horizontal axis is normalized by the fiber radius, 375 μm) at 0.65- μm wavelength.

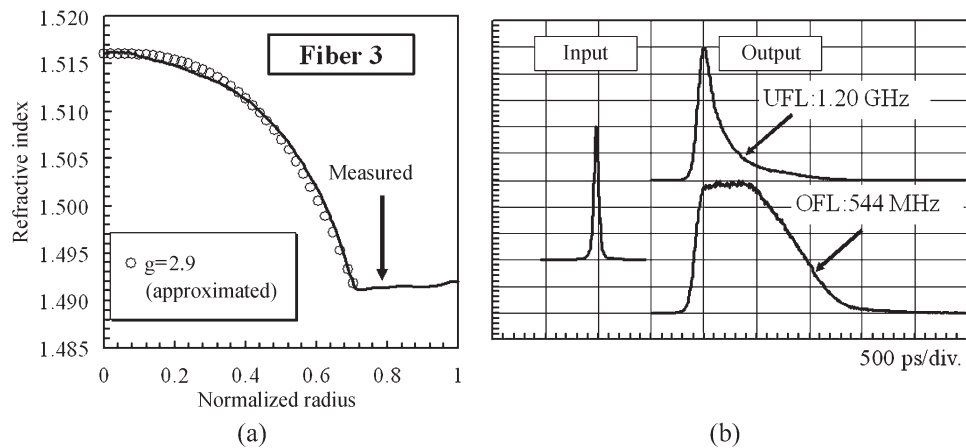


Fig. 5. (a) Refractive-index profiles of the GI POFs with the same index exponent and different NA. (b) Comparison of the output-pulse waveforms from two GI POFs for 100-m transmission.

544 MHz and 1.20 GHz, respectively, as shown in Fig. 5(b). The bandwidth can be improved significantly by adopting the UFL condition.

Next, we propose a new refractive-index profile for the UFL condition. The new index profile is not necessarily approximated by a single index exponent g . In this paper, the bandwidth performance of the GI POF with the new refractive-index profile is investigated by varying the launch conditions. Two representative refractive-index profiles are shown in Fig. 6(a) and (c) (fiber 4 and fiber 5, respectively), where the profiles only near the core center are approximated by a small g value (1.9, 2.3), while larger g values (3.5, 3.8) are required for fitting the index at the periphery region. The bandwidth of the 100-m fiber 4 and fiber 5 under OFL and UFL conditions at a wavelength of 0.65 μm are measured, as shown in Fig. 7(b) and (d), respectively. In fiber 4, although the bandwidth under OFL is 883 MHz, it is improved to 2.14 GHz under UFL, which is almost twice as high as the bandwidth under OFL. In Fig. 6(d), the bandwidth of fiber 5 under UFL and OFL are 577 MHz and 2.44 GHz, respectively, where a larger difference is observed in the bandwidth under UFL and OFL than that of fiber 4.

This new index profile can be obtained substantially more easily by the interfacial-gel polymerization process only by decreasing the polymerization temperature below 100 $^{\circ}\text{C}$. Since the boiling point of the monomer of PMMA is approximately 100 $^{\circ}\text{C}$, high pressure is required if the polymerization temperature is higher than 100 $^{\circ}\text{C}$. Therefore, the low polymerization temperature simplifies the fabrication setup of GI preforms. The polymerization-temperature dependence of the index profile formed in the PMMA-based GI POF is shown in Fig. 7. The concentrations of monomer, dopant, polymerization initiator, and chain-transfer agent for these GI preforms are the same, while only the polymerization temperature is different. The measured refractive-index profile formed by the high polymerization temperature (120 $^{\circ}\text{C}$) is well fitted to the power-law form ($g = 4.3$) in the entire core region as shown in Fig. 7(a). On the other hand, the profile obtained by the low polymerization temperature (90 $^{\circ}\text{C}$) deviates from the power-law form as shown in Fig. 7(b), which is a very similar profile to that of fiber 4 [Fig. 6(a)]. However, the index profile formed by the high polymerization temperature, as shown in Fig. 7(a), is approximated by a larger g value because of the high

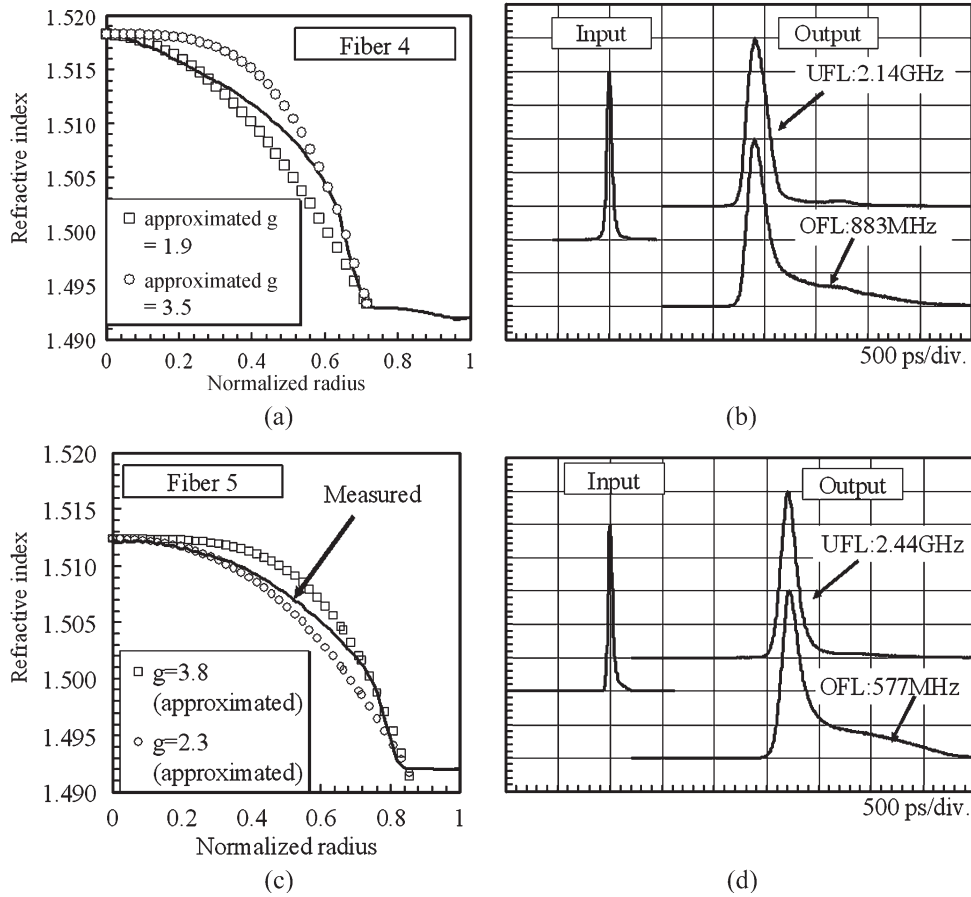


Fig. 6. Measured refractive-index profile and output-pulse waveforms from 100-m fiber 4 (NA = 0.28, horizontal axis is normalized by fiber radius, 250 μm) and fiber 5 (NA = 0.26, horizontal axis is normalized by the fiber radius, 250 μm) at 0.65- μm wavelength. (a) Refractive-index profile of fiber 4. (b) Input- and output-pulse waveforms and -3-dB bandwidth of fiber 4. (c) Refractive-index profile of fiber 5. (d) Input- and output-pulse waveforms and -3-dB bandwidth of fiber 5.

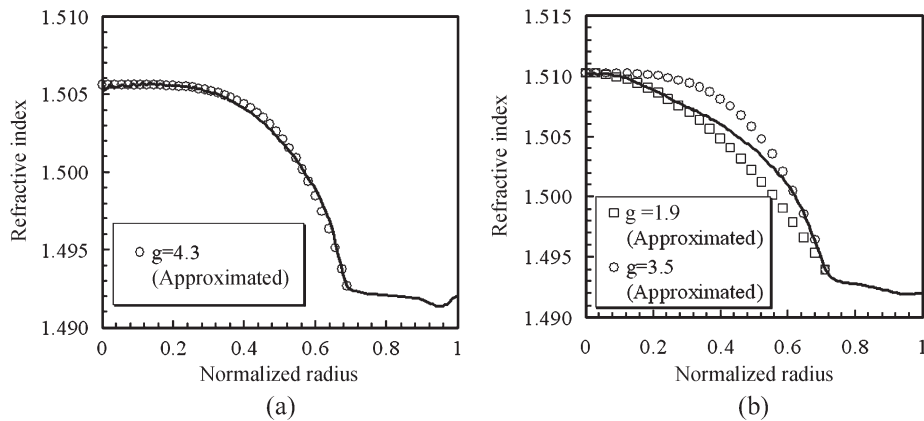


Fig. 7. (a) Measured refractive-index profile formed by high polymerization temperature (120 $^{\circ}\text{C}$). Horizontal axis is normalized by the fiber radius 375 μm . (b) Measured refractive-index profile formed by low polymerization temperature (90 $^{\circ}\text{C}$). Horizontal axis is normalized by the fiber radius 375 μm .

polymerization rate [6]. We are investigating why the index profile tends to deviate from the power-law form when polymerized under 100 $^{\circ}\text{C}$. The results of a detailed analysis will be described in the other papers.

C. Group Delay Analysis

To investigate the modal properties of fiber 3 and fiber 4, the group delay of each mode in these fibers is analyzed by

measuring the DMD. The DMD with respect to the normalized principal mode number (m/M) shown by (5) is measured

$$\frac{m}{M} = \left(\frac{r}{a}\right)^{\frac{(g+2)}{2}} \tag{5}$$

where r is the distance from the core center to the position where the single-mode fiber is butted.

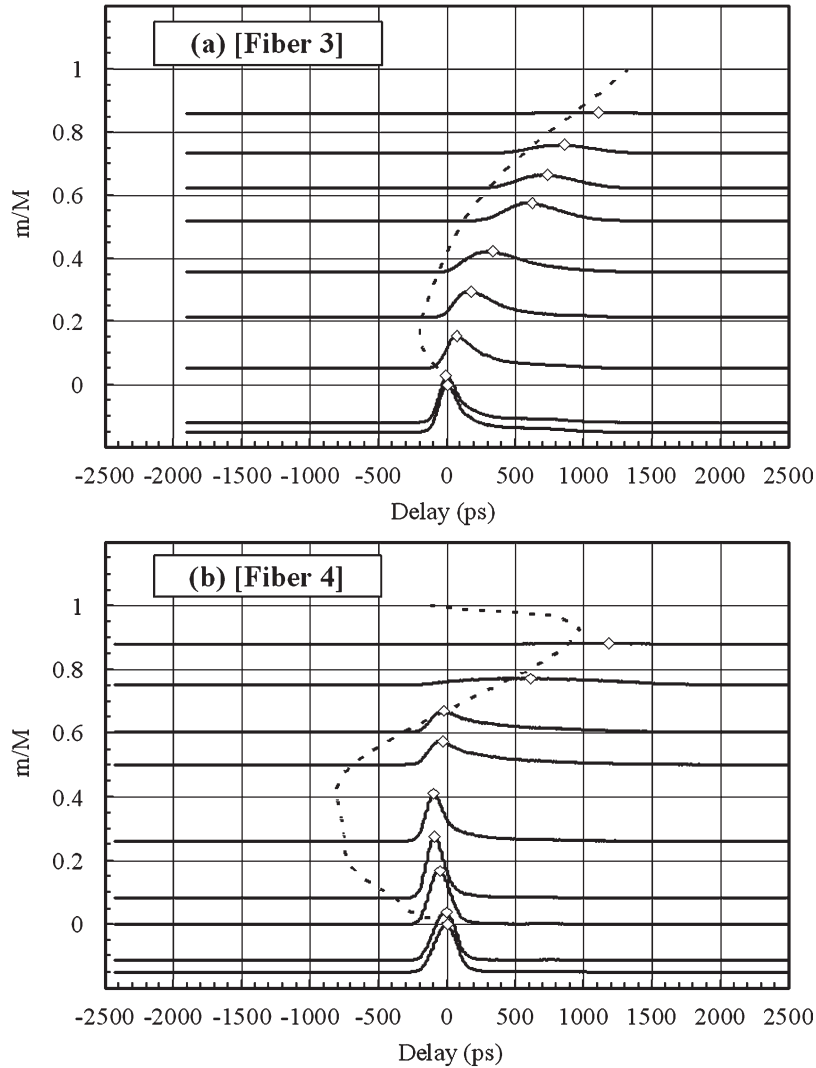


Fig. 8. Measured DMD after 100-m transmission through (a) fiber 3 and (b) fiber 4 at 0.65- μ m wavelength. Broken line: calculated DMD.

The results of the DMD measurement in the 100-m fiber 3 and fiber 4 are shown in Fig. 8(a) and (b), respectively. The DMD is theoretically calculated by the WKB method from the measured refractive-index profile [8]. In these calculations, the index profiles of the fibers were approximated by the ten-term polynomial form described by (3). The calculated group delay of fiber 3, the refractive-index profile of which is shown in Fig. 5(a), is plotted in Fig. 8(a) by a broken line and is compared to the measured results, with the DMD of only meridional modes (with azimuthal mode-number zero). In Fig. 8(a), the measured DMD values shown by the peak position in each pulse (open diamond) monotonically increase with increasing normalized principal mode number in almost the same manner as the calculated group delay. Here, the vertical position of each pulse shown in Fig. 8 is adjusted to show that the peak of the pulse (plotted by open diamonds) can indicate the group delay of each mode with the normalized principal mode number in the vertical axis.

On the other hand, the calculated group delay of fiber 4, the refractive-index profile of which is shown in Fig. 6(a), is plotted in Fig. 8(b) compared to the measured results in the same manner as Fig. 8(a). In Fig. 8(b), almost the same

delay times are measured over the normalized principal mode number range of 0 to 0.7. In contrast, the calculated DMD curve shows positive and negative delay times for low- and high-order modes, respectively, and two turning points are observed at -800 and $+1000$ ps. With the normalized principal mode number within the range of 0 to 0.6, a negative time delay is predicted by the theoretical calculation, because the approximated g value (1.9) around the core center is smaller than optimum $g = 2.4$, which indicates overcompensation of the modal dispersion. However, this negative time delay is only barely observed in the experimental results, and is not as large as predicted by the calculated result. In these lower order modes, even if a small spot from the single-mode fiber is used for a selective launch, several modes (a mode group) must be simultaneously launched, which would have characteristics which are the average of the launched modes. This multiple-mode group launch is confirmed by the NFP profiles of a center launch shown in Fig. 2, where optical output is observed even at the periphery region of the core. The broad NFP profile of the center launch in Fig. 2 may be regarded as a result of mode coupling. However, we have already confirmed in [19] that the similar NFP profile of the center launch is also

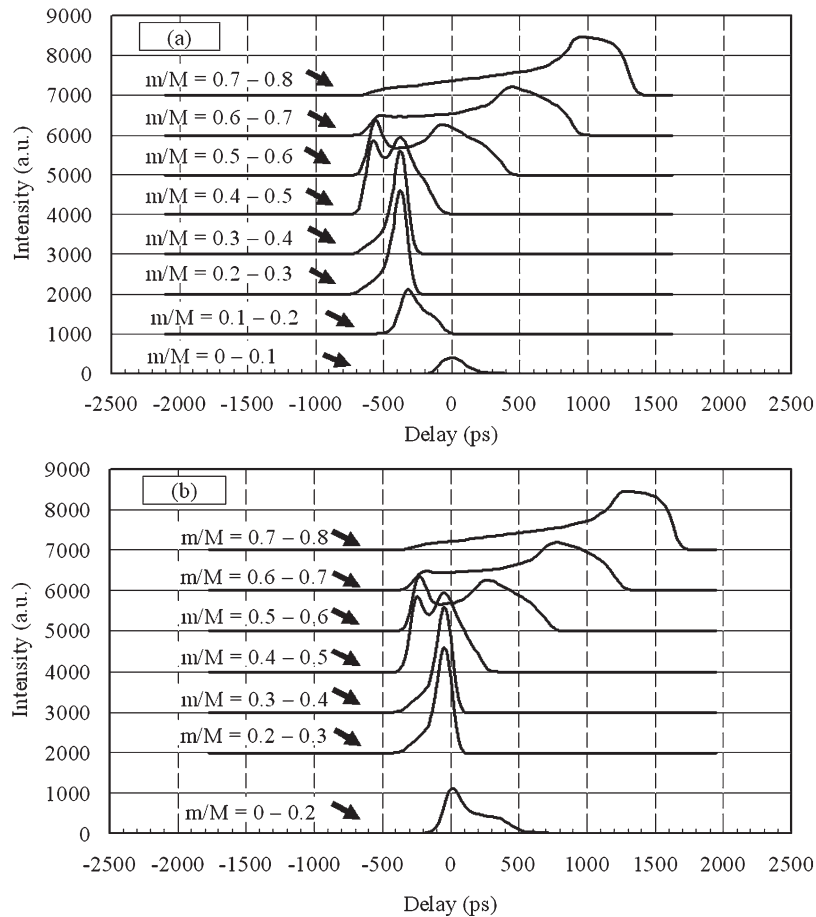


Fig. 9. Calculated DMD after 100-m transmission through fiber 4 by assuming several mode groups are simultaneously launched by the single-mode fiber probe. (a) Mode groups of $0 < m/M < 0.1$ are assumed to be excited by the center launch. (b) Mode groups of $0 < m/M < 0.2$ are assumed to be excited by the center launch.

observed even for a short-distance (5 m) GI POF. Therefore, the broad NFP is likely not the result of mode coupling. At the coupling point between the single-mode-fiber probe and the GI POF, a small amount of optical power might be coupled to intermediate-order modes because of the mode-power-profile difference between the single-mode fiber and GI POF. This power-coupling issue is under investigation because it is very important, particularly for the design of optical transmitters for GI POFs. The results will be described in another article. Thus, even if the single-mode-fiber position is scanned from the core center to selectively launch as small number of modes as possible, the obtained delay time shows a somewhat-averaged value among the several of tens of launched modes. That is why the experimental DMD results show disagreement with the calculated curve in Fig. 8(b).

In order to confirm the cause of the disagreement mentioned above, the calculated DMD waveforms of fiber 4 are shown in Fig. 9(a), where a small mode group of the GI POF is supposed to be launched by the output signal from the single-mode-fiber probe. These waveforms are obtained by convolving the experimentally measured input pulse with the calculated impulse-response function of each mode group. Since the differential mode attenuation is not taken into consideration, the intensity of the higher order mode groups are much stronger than the experimentally measured intensity of the corresponding high-

order modes shown in Fig. 8(b). In this case, the group delay of each mode (peak position of each waveform) is similar to the broken line in Fig. 8(b).

On the other hand, the calculated DMD waveforms of fiber 4 are also shown in Fig. 9(b), where the modes with m/M from 0 to 0.2 are assumed to be launched by the center launch of single-mode fiber. According to this assumption, the negative time delays of intermediate modes ($0.2 < m/M < 0.8$) should be contracted compared to the delay of corresponding modes in Fig. 9(a). The calculated results of DMD shown in Fig. 9(b) are close to the measured results shown in Fig. 8(b). Therefore, the discrepancy of the measured and calculated DMDs can be explained by the averaged group delay of several modes.

From the group-delay analysis by the WKB numerical calculation and the DMD measurement, we demonstrate that the combined profile with index exponents lower and higher than the optimum value for the core center and periphery, respectively, is more effective for high-bandwidth performance under the UFL condition than other profiles, although the completely ideal one ($g = 2.4$) is the exception. Moreover, we also verify that, for the profile near the core center, a g value smaller than 2.4 (optimum) is more effective for high bandwidth under UFL, because the optical power of only low-order modes can be more tightly confined near the core center when the g value is smaller than optimum. This confinement efficiency of the

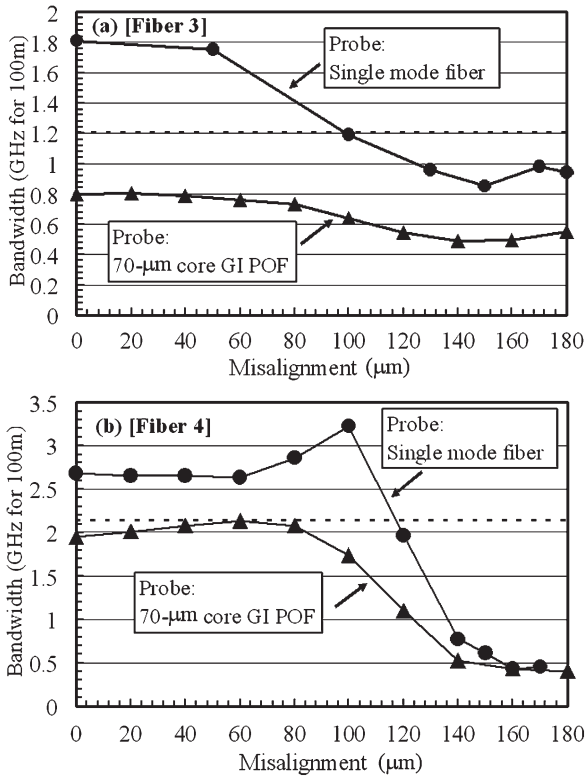


Fig. 10. Measured bandwidths for 100-m fiber 3 and fiber 4 with misalignment at the coupling between the probe fiber and the tested GI POF. Broken line: bandwidth launched by the typical LD-based transmitter (UFL) with lens optics.

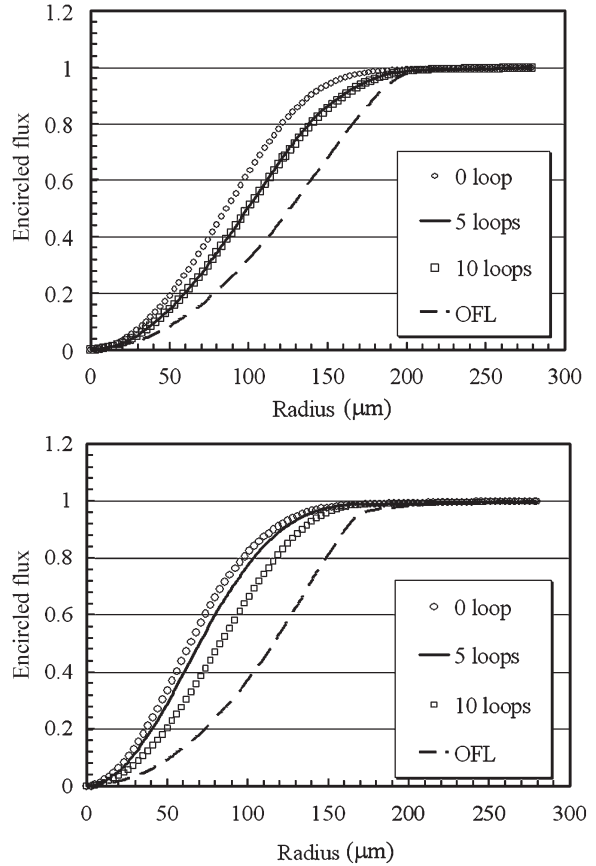


Fig. 12. EF from 100-m fiber 3 and fiber 4 launched by single-mode silica fiber at the core center with fiber bending present. Broken line: bandwidth under the OFL condition.

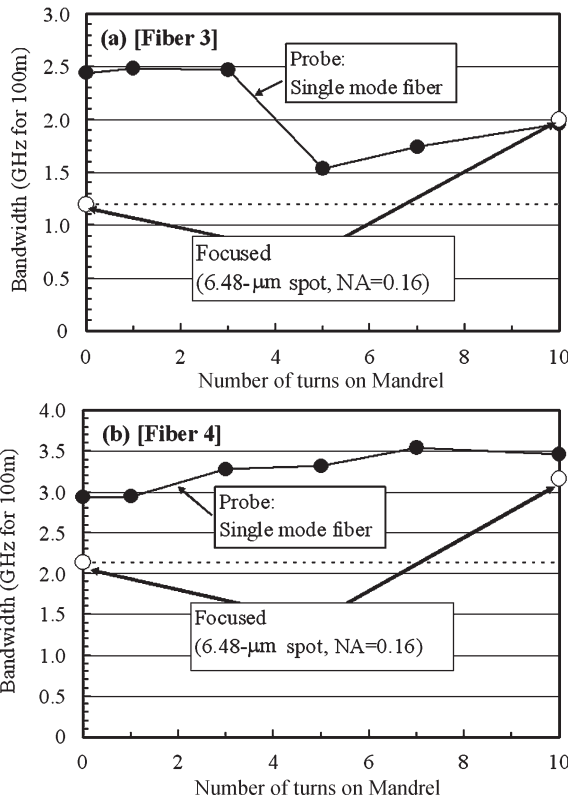


Fig. 11. Measured bandwidths at 0.65-μm wavelength for 100-m fiber 3 and fiber 4 with multiple fiber bendings. Broken line: bandwidth launched by the typical LD-based transmitter (UFL) with lens optics.

optical power of low-order modes is investigated and mentioned in Section III-D.

D. Stability of High-Bandwidth Performance Under Perturbations in Very-Short-Reach Networks

The measured bandwidth of 100-m fiber 3 and fiber 4, with misalignment between the probe and tested fibers at the launching position, are shown in Fig. 10. It is found that the bandwidth performance depends on the type of probe fiber, particularly in fiber 3, the index profile of which is described by a single index exponent. In the case of fiber 3, large bandwidth degradation is observed when the launching spot size is large compared to that of the single-mode-fiber launch. Furthermore, the bandwidth gradually decreases with increasing misalignment in both launch conditions. On the other hand, the launch-condition dependence (probe dependence) is small in fiber 4 as shown in Fig. 10(b). The high-bandwidth performance in fiber 4 is maintained even with a 80-μm misalignment, for both launch conditions. These results indicate that a large tolerance in the optics design is allowed in the transmitter for fiber 4.

The effect of static fiber bending on the bandwidth performance is investigated. The results are shown in Fig. 11. The bandwidth of fiber 4 shows little change after multiple bendings as shown in Fig. 11(b), when a pulse is launched by the single-mode-fiber probe and the typical LD-based transmitter (UFL) with lens optics (spot size: 6.48 μm, NA: 0.16). On the other

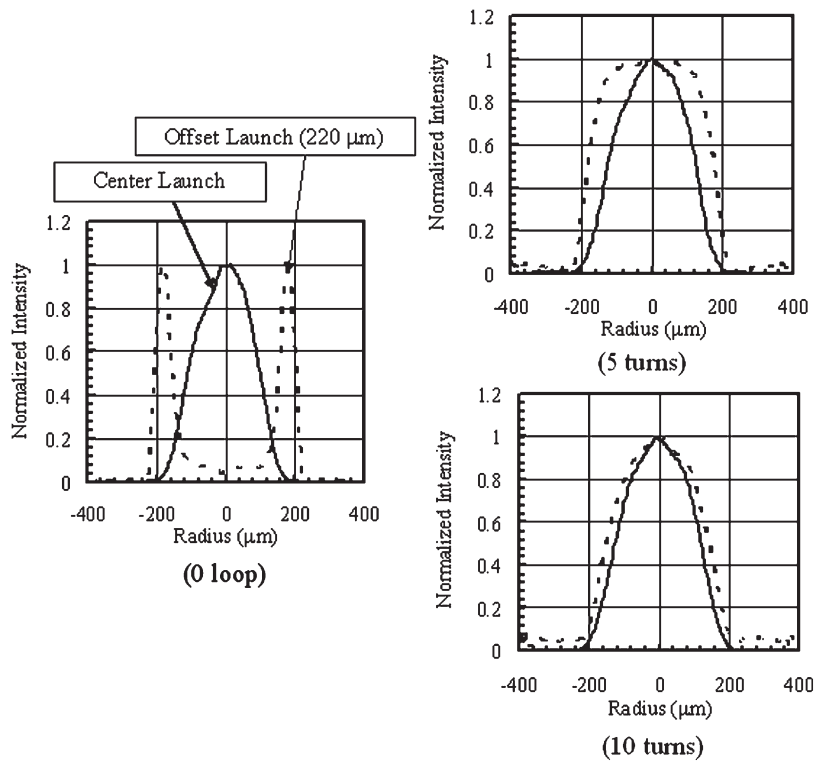


Fig. 13. Measured NFPs of low- and high-order modes from 100-m fiber 3 as a function of bending-loop number.

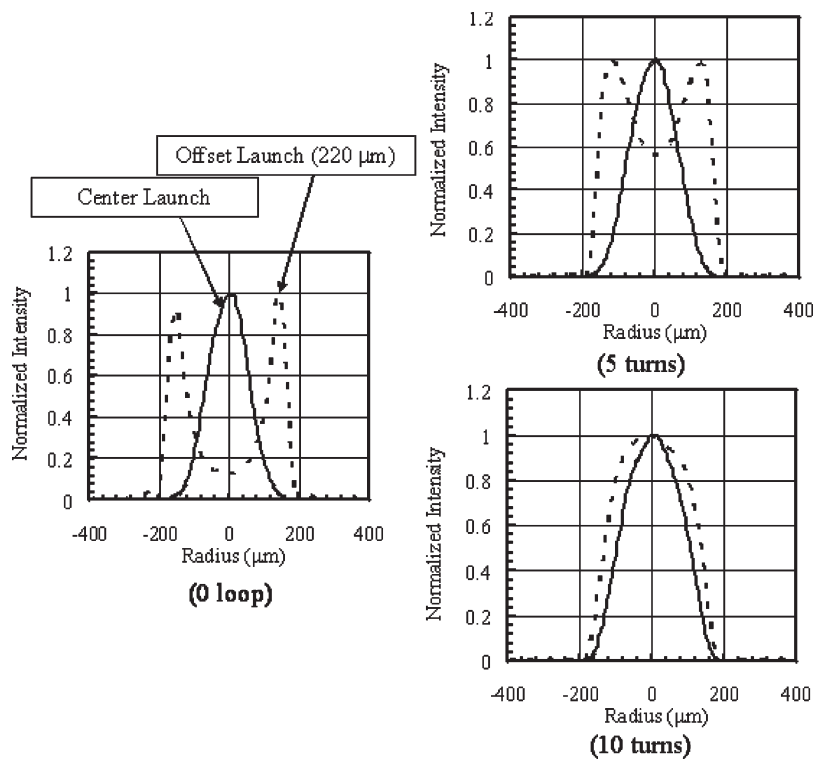


Fig. 14. Measured NFPs of low- and high-order modes from 100-m fiber 4 as a function of bending-loop number.

hand, large bandwidth degradation is observed in fiber 3 when the number of turns is increased to between three and five, as shown in Fig. 11(a). Thus, it is found that even tight fiber bending does not change the high-bandwidth performance of the GI POF with the new index profile mentioned above.

On the other hand, the mode-power distribution after multiple bendings is shown in Fig. 12, where it is described using encircled flux (EF) calculated from a two-dimensional near-field pattern [20]. EFs indicate the normalized total optical power propagating in MMF as a function of the fiber radius.

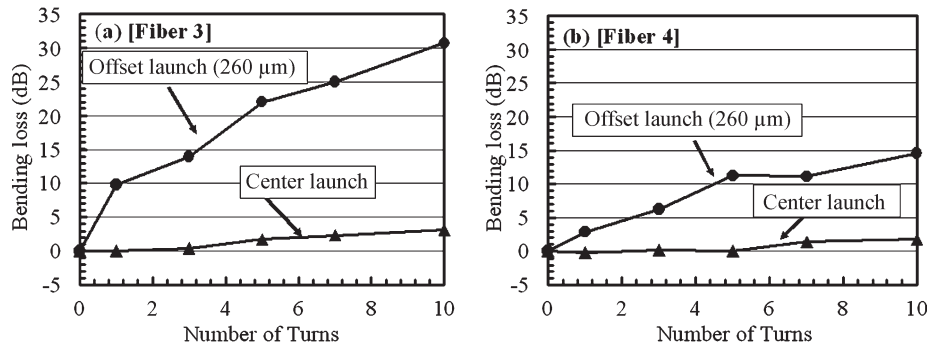


Fig. 15. Measured bending losses of (a) fiber 3 and (b) fiber 4 under center and offset launch conditions as a function of bending-loop number. Wavelength = 0.65 μm .

It is found in Fig. 12 that optical power diffuses from low- to high-order modes with an increase in the number of turns in both fibers. However, the mode power does not completely diffuse to the broken line that is observed under the OFL condition. Therefore, the mode power does not diffuse to the highest order mode even under the most severe bending condition (~ 10 turns).

The launch-condition dependencies of the NFP with no bending and after multiple bendings of 100-m fiber 3 and fiber 4 are also measured as shown in Figs. 13 and 14, respectively. The measured NFPs for both fibers show that each mode group independently propagates before bending because mode coupling is reduced by adjusting their NAs, as mentioned above. On the other hand, each mode group in both fibers does not independently propagate after the severe bending (ten turns) for either fiber. The measured NFPs after five-turn bending show that the launch-condition dependence in fiber 4 (Fig. 14) is clearer than that in fiber 3 (Fig. 13). These results indicate that the mode-coupling strength in fiber 4 from low- order to high-order modes under multiple bendings is smaller than that in fiber 3.

However, the optical loss due to the static fiber bending is also of great concern. Fig. 15(a) and (b) show the mode-group-dependent bending loss of fiber 3 and fiber 4, respectively. The same single-mode-fiber launch condition as those shown in Fig. 11 is used, and the output-power losses for center launch and 260- μm offset launch are measured before and after fiber bendings using an optical power meter. As shown in Fig. 15(a) and (b), both lower and higher order mode groups are well confined in fiber 4 compared to those in fiber 3. This lower bending loss in fiber 4 is also explained by the small mode coupling. In fiber 4, each mode group independently propagates without mode coupling. Therefore, the power coupling from these guided modes to radiation modes are also small.

This difference in the mode-coupling strength can be evaluated by $\Delta\beta$ values. Each $\Delta\beta$ value of the modes propagating in fiber 3 and fiber 4 is shown in Fig. 16. These $\Delta\beta$ values are numerically calculated by approximating the refractive-index profile of the core by the ten-term polynomial of (3). It can be seen that the curve of the $\Delta\beta$ values of fiber 4 is V-shaped, and the $\Delta\beta$ values of fiber 4 are higher than those of fiber 3 in almost all of the modes. Calculated $\Delta\beta$ values of the GI POFs with power-law profiles ($g = 1.5, 2.0,$ and 3.0) are shown in Fig. 17. The $\Delta\beta$ value monotonically increases with

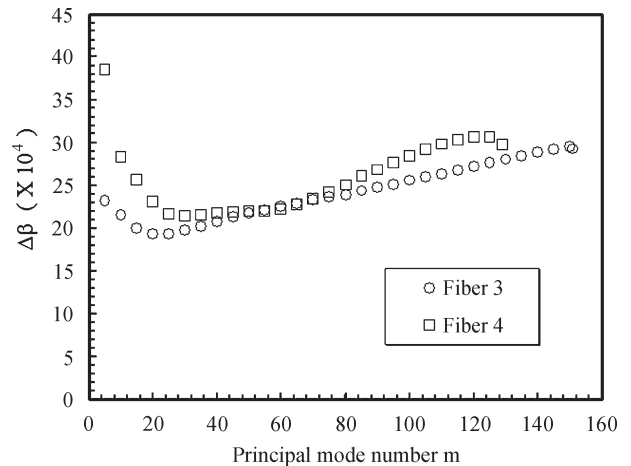


Fig. 16. Difference between propagation constants ($\Delta\beta$) of adjacent modes in fiber 3 and fiber 4.

increasing principal mode number when g is larger than 2.0, and monotonically decreases with g smaller than 2.0. In addition, when g is just 2.0, the $\Delta\beta$ value is almost uniform in all the modes. From these results, it is found that the low-order modes tend not to couple to intermediate and high-order modes in the GI POF with g smaller than 2.0. This is the reason why the core center should be fitted to a g value smaller than optimum mentioned in Section III-C. Because of the combined profile of different g values, $\Delta\beta$ of high-order modes take on larger values. The V-shaped $\Delta\beta$ values in fiber 4 are attributed to the combined profile with the index exponents lower and higher than optimum for the core center and periphery, respectively, as shown in Fig. 6. Particularly, $\Delta\beta$ of the low-order modes ($0 < \text{principal mode number} < 20$) shows extremely large values such as 30×10^4 to 40×10^4 .

We show in Fig. 3 that the high-NA GI POFs with the $\Delta\beta$ values larger than 15×10^4 exhibit weak mode coupling. Compared to those GI POFs, it can be seen that the $\Delta\beta$ values of the low-order modes for fiber 4 are large enough for suppressing mode coupling. Therefore, a large $\Delta\beta$ value in all the modes is considered to be the reason why small mode coupling is observed in fiber 4, even after five bending turns. It was verified that the new index-profile design mentioned above could confine the optical power of low-order modes launched by the UFL condition in the core center more efficiently than other index profiles.

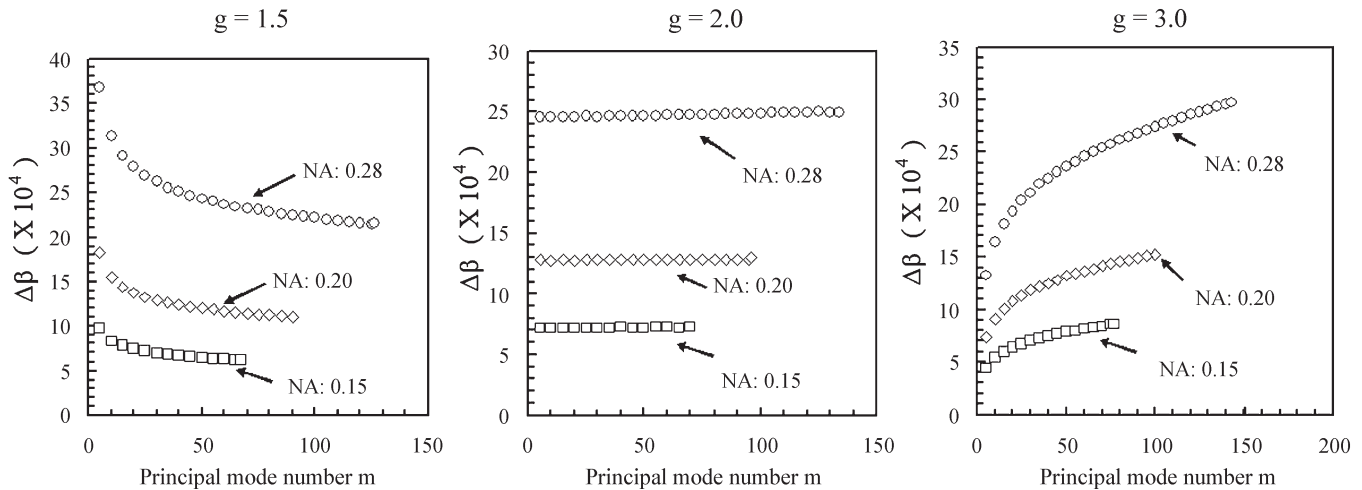


Fig. 17. Difference between propagation constants ($\Delta\beta$) of adjacent modes in GI POFs having various power-law forms ($g = 1.5, 2.0,$ and 3.0).

IV. CONCLUSION

In this paper, we verified that the numerical aperture (NA) of graded-index plastic optical fibers (GI POFs) is a key factor in mode-coupling strength; consequently, the amount of mode coupling can be controlled by adjusting the NA of GI POFs. Furthermore, we proposed a new index-profile design for high-bandwidth performance under the under-filled launch (UFL) condition. It was also confirmed that the high bandwidth of the GI POF with the new index profile mentioned above could be maintained even if some perturbations are caused, such as misalignment between the light source and the fiber at the light coupling or fiber bending, which are common in very-short-reach networks.

REFERENCES

- [1] P. Pepeljugoski, D. Kuchta, Y. Kwark, P. Pleunis, and G. Kuyt, "15.6-Gb/s transmission over 1 km of next generation multimode fiber," *IEEE Photon. Technol. Lett.*, vol. 14, no. 5, pp. 717–719, May 2002.
- [2] J. Goudeau, G. Widawski, M. Rossbach, B. Bareel, R. Helvenstein, and L. Huff, "GI POF for Gb ethernet links," in *Proc. 13th Int. Plastic Optical Fibre Conf.*, Nürnberg, Germany, Sep. 2004, pp. 76–81.
- [3] A. M. J. Koonen, H. van den Boom, L. Bakker, J. Zeng, and G. D. Khoe, "Integration of services in short-range multimode polymer optical fibre networks by exploiting the higher-order fibre passbands," in *Proc. 13th Int. Plastic Optical Fibre Conf.*, Nürnberg, Germany, Sep. 2004, pp. 90–97.
- [4] S. Junger, M. Schrader, A. Ploetz, W. Tschekalinskij, and N. Weber, "High linearity CATV transmission with GI-POF and SI-POF," in *Proc. 13th Int. Plastic Optical Fibre Conf.*, Nürnberg, Germany, Sep. 2004, pp. 106–112.
- [5] T. Ishigure, E. Nihei, and Y. Koike, "Graded-index polymer optical fiber for high speed data communication," *Appl. Opt.*, vol. 33, no. 19, pp. 4261–4266, Jul. 1994.
- [6] T. Ishigure, M. Sato, O. Takanashi, E. Nihei, T. Nyu, S. Yamazaki, and Y. Koike, "Formation of the refractive index profile in the graded index polymer optical fiber for gigabit data transmission," *J. Lightw. Technol.*, vol. 15, no. 11, pp. 2095–2100, Nov. 1997.
- [7] T. Ishigure, Y. Koike, and J. W. Fleming, "Optimum index profile of the perfluorinated polymer based GI polymer optical fiber and its dispersion properties," *J. Lightw. Technol.*, vol. 18, no. 2, pp. 178–184, Feb. 2000.
- [8] T. Ishigure, S. Tanaka, E. Kobayashi, and Y. Koike, "Accurate refractive index profiling in a graded-index plastic optical fiber exceeding gigabit transmission rates," *J. Lightw. Technol.*, vol. 20, no. 8, pp. 1449–1556, Aug. 2002.
- [9] S. Takahashi, "Experimental studies on launching conditions in evaluating transmission characteristics of POFs," in *Proc. Plastic Optical Fiber (POF)*, The Hague, The Netherlands, 1993, pp. 83–85.
- [10] A. F. Garito, J. Wang, and R. Gao, "Effects of random perturbations in plastic optical fibers," *Science*, vol. 281, no. 5379, pp. 962–967, Aug. 1998.
- [11] T. Ishigure, M. Kano, and Y. Koike, "Which is a more serious factor to the bandwidth of GI POF: Differential mode attenuation or mode coupling?," *J. Lightw. Technol.*, vol. 18, no. 7, pp. 959–965, Jul. 2000.
- [12] S. E. Golowich, W. White, W. A. Reed, and E. Knudsen, "Quantitative estimates of mode coupling and differential modal attenuation in perfluorinated graded-index plastic optical fiber," *J. Lightw. Technol.*, vol. 21, no. 1, pp. 111–121, Jan. 2003.
- [13] D. Marcuse, "Mode mixing with reduced losses in parabolic-index fibers," *Bell Syst. Tech. J.*, vol. 55, no. 6, pp. 777–802, Jun. 1976.
- [14] Y. Ohtsuka and Y. Koike, "Determination of the refractive-index profile of light-focusing rods: Accuracy of a method using Interphako interference microscopy," *Appl. Opt.*, vol. 19, no. 16, pp. 2866–2872, Aug. 1980.
- [15] D. Marcuse, *Principles of Optical Fiber Measurements*. New York: Academic, 1981.
- [16] —, "Coupled mode theory of round optical fiber," *Bell Syst. Tech. J.*, vol. 52, no. 6, pp. 817–842, Jun. 1973.
- [17] D. G. Cunningham, W. G. Lane, and B. Lane, *Gigabit Ethernet Networking*. Indianapolis, IN: Macmillan, 1999.
- [18] L. Raddatz, I. H. White, D. G. Cunningham, and M. C. Nowell, "An experimental and theoretical study of the offset launch technique for the enhancement of the bandwidth of multimode fiber links," *J. Lightw. Technol.*, vol. 16, no. 3, pp. 324–331, Mar. 1998.
- [19] K. Ohdoko, T. Ishigure, and Y. Koike, "Propagating mode analysis and design of waveguide parameters of GI POF for very short-reach network use," *IEEE Photon. Technol. Lett.*, vol. 17, no. 1, pp. 79–81, Jan. 2005.
- [20] *FOTP-203—launched power distribution measurement procedure for graded-index multimode fiber transmitters*, TIA/EIA-455-203, Jun. 2001.



Takaaki Ishigure (M'00) was born in Gifu, Japan, on July 30, 1968. He received the B.S. degree in applied chemistry and the M.S. and Ph.D. degrees in material science from Keio University, Yokohama, Japan, in 1991, 1993, and 1996, respectively. He is currently an Assistant Professor of Keio University. He has been, concurrently, a Group Leader of the Japan Science and Technology Agency (JST) Exploratory Research for Advanced Technology (ERATO) "Koike Photonics Polymer Project." In 2005, he joined the Department of Electrical Engineering, Columbia University, New York, as a Visiting Research Scientist. His current research interests are in the preparation of high-bandwidth graded-index polymer optical fiber and its system design.



Kunihiko Ohdoko was born in Tokyo, Japan, on October 14, 1979. He received the B.S. degree in applied physics and physico-informatics and the M.S. degree in integrated design engineering from Keio University, Yokohama, Japan, in 2003 and 2005, respectively.

He is with Sumitomo Mitsui Banking Corporation (SMBC) Consulting Company, Ltd., Tokyo, Japan.



Yorichika Ishiyama was born in Kanagawa, Japan, on November 11, 1982. He received the B.S. degree in applied physics and physico-informatics from Keio University, Yokohama, Japan, in 2005. He is currently pursuing the master's degree in integrated design engineering from Keio University.

He is currently interested in research on propagating-mode analysis in graded-index plastic optical fibers (GI POFs).



Yasuhiro Koike (M'02–A'02–M'03) was born in Nagano, Japan, on April 7, 1954. He received the B.S., M.S., and Ph.D. degrees in applied chemistry from Keio University, Yokohama, Japan, in 1977, 1979, and 1982, respectively.

He has been a Professor of Keio University, Japan, and developed the high-bandwidth graded-index polymer optical fiber (GI POF). He has been concurrently the Director of the Japan Science and Technology Agency (JST) Exploratory Research for Advanced Technology (ERATO) "Koike Photonics Polymer Project" since 2000. He stayed as a Visiting Researcher at American Telephone and Telegraph (AT&T) Bell Laboratories from 1989 through 1990.

Dr. Koike received the International Engineering and Technology Award of the Society of Plastics Engineers, in 1994, and the Fujiwara Award in 2001.